Direct Measurements of Hydrophobic Slippage Using Double-Focus Fluorescence Cross-Correlation

Olga I. Vinogradova,[1] Kaloian Koynov,[2] Andreas Best,[2] and François Feuillebois[3]

[1]*A.N. Frumkin Institute of Physical Chemistry and Electrochemistry, Russian Academy of Sciences, 31 Leninsky Prospect, 119991 Moscow, Russia*

[2]*Max Planck Institute for Polymer Research, Ackermannweg 10, 55128 Mainz, Germany*

[3]*PMMH, CNRS UMR 7636, ESPCI, 10 rue Vauquelin, 75231 Paris Cedex 05, France*

(Received 29 January 2008; published 20 March 2009)

We report the results of direct measurements of velocity profiles in a microchannel with hydrophobic and hydrophilic walls, using a new high-precision method of double-focus spatial fluorescence cross correlation under a confocal microscope. In the vicinity of both walls the measured velocity profiles do not go to zero by supplying a plateau of constant velocity. This apparent slip is proven to be due to a Taylor dispersion, an augmentation by shear diffusion of nanotracers in the direction of flow. Comparing the velocity profiles near the hydrophobic and hydrophilic walls for various conditions shows that there is a true slip length due to hydrophobicity. This length, of the order of several tens of nanometers, is independent of the electrolyte concentration and shear rate.

DOI: 10.1103/PhysRevLett.102.118302 PACS numbers: 83.50.Rp, 68.08.−p, 82.70.Dd, 83.50.Lh

For more than a hundred years, scientists and engineers have assumed and successfully applied no-slip boundary conditions to model experiments in fluid mechanics. However, recently it has been well recognized that the success of this famous postulate reflected mostly a macroscopic character and insensitivity of old experiments. Reducing the size of systems to micro- and nanodimensional led to a conclusion that the no-slip condition does not always apply [1]. It is now clear that many systems should allow for an amount of slippage, described by the condition $v_s = b\partial v/\partial z$ (or its tensorial generalization [2]), where v_s is the slip velocity at the wall and the axis z is normal to the surface. What, however, remains a matter of debate is the amplitude of the slip, and its variation with interfacial properties and parameters of the flow.

From the theoretical point of view, slippage should not appear on a hydrophilic surface, except as at a very high shear rate [3]. A slip length of the order of a hundred nanometers or smaller is, however, expected for a hydrophobic surface [4–6]. On the experimental side, no consensus has been achieved so far. While some experimental data are consistent with the theoretical expectations both for hydrophilic [7–11] and hydrophobic surfaces [7–9,12], some other reports completely escape from this picture with both quantitative (slippage over hydrophilic surface, shear rate dependent slippage, rate threshold for slip, etc.) and quantitative (slip length of several μms) discrepancies (for a recent review see [13]). Clearly, in order to rationalize the situation, new data, preferably obtained with a new experimental technique, are necessary.

Basically, two types of experimental methods were used to study boundary conditions. High-speed force measurements performed with the surface forces apparatus [8,14] or atomic force microscope [7] allow to deduce a drag force, with the subsequent comparison with a theory of a film drainage [4]. This approach, being extremely accurate at the nanoscale, does not provide visualization of the flow profile, so that these measurements are identified as indirect. Direct approaches to flow profiling, or velocimetry, take advantage of various optics to monitor tracer particles [15–17]. Their accuracy is normally much lower than that of force methods due to relatively low optical resolution, system noise due to polydispersity of tracers, and difficulties in decoupling flow from diffusion. As a consequence, it is normally expected that a slippage of the order of a few tens of nanometers cannot be detected by a velocimetry technique.

In this Letter, we report direct high-precision measurements at the nanoscale performed with a new optical technique. As an alternative to the existing TIR-FRAP [15], μPIV [16,17], and TIRV [12] methods, here we use a new technique, based on a double-focus spatial fluorescence cross correlation (DF-FCS) [18]. Results obtained for various concentrations of added salt and wettability of substrates lead to apparent slip lengths (velocity of tracers) on both hydrophilic and hydrophobic surfaces, and measurable differences between them. We quantify the tracer distribution in the flow field and show that it is affected by Taylor dispersion. This allows us to confirm the no-slip condition past a hydrophilic surface, and to deduce the true hydrophobic slip length.

Our microchannel was formed by a three-layer sandwich construction. The lowest layer was a standard microscope cover slide made of borosilicate glass. The root-mean-square roughness measured by an atomic force microscope was in the range of 0.3 nm. The water advancing contact angle on this slide was measured to be below 5°. The channel itself was created by cutting out a hole in an

adhesive polymer film (Tessa, Germany) with a thickness of around 100 μm, that forms the smallest dimension of the channel, directed along the z axis. The top layer was formed by a cover glass. Its surface was made hydrophobic by treatment by a vapor of trimethylchlorosilane. After silanization, the water advancing contact angle was 95° and the root-mean-square roughness was below 0.7 nm. A hydrostatic pressure gradient was created by two beakers of different heights, which allowed us to vary a shear rate near the wall in the range $\lambda = 800$–$3000\ s^{-1}$. As tracers we used carboxylate-modified latex FluoSpheres 580/605 of a radius of $R \sim 20$ nm, (Molecular Probes, Eugene, Oregon). Experiments were carried out in water and NaCl aqueous solutions with concentrations in the range between 10^{-5} mol/L and 10^{-2} mol/L.

The scheme of the DF-FCS method was described in detail in [18]. Briefly, we used a commercial FCS setup (Carl Zeiss, Jena, Germany) consisting of the module ConfoCor 2 and the inverted microscope model Axiovert 200. For the present experiments, we employed a water immersion objective (Zeiss, C-Apochromat 40 ×, NA 1.2). The optical system was modified so that an external laser beam could be coupled into the confocal optics. For fluorescence excitation, the 543-nm line of a 1-mW helium-neon laser was used. The laser beam was split by means of a Wollaston prism. Behind the prism, the two beams are polarized perpendicularly to each other and exhibit an angular separation of 0.5°. After passing through two additional lenses, these beams are fed into the confocal microscope. Our alignments result in two optically equivalent, almost diffraction-limited laser foci (diameter ~400 nm, height ~3 μm) separated by a distance of 6.0 ± 0.1 μm in object space as is schematically shown in Fig. 1. As the fluorescence tracers are flowing along the channel, they are crossing consecutively the two foci, producing two time-resolved fluorescence intensities $I_1(t)$ and $I_2(t)$ recorded independently from the avalanche photo diodes. The time cross correlation function can be calculated as $G(\tau) = \langle I_1(t) I_2(t+\tau)\rangle_t / \langle I_1(t)\rangle_t \langle I_2(t)\rangle_t$ and typically exhibits a local maximum. The position of this maximum τ_M is characteristic of the local velocity of the tracers.

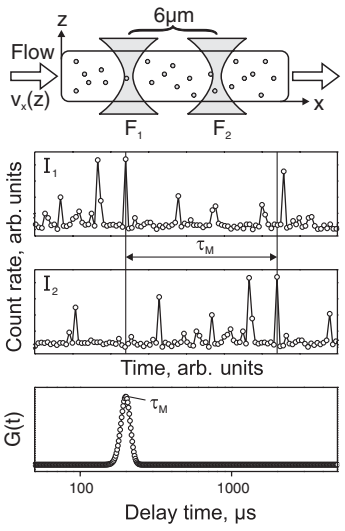

FIG. 1. Schematics of the DF-FCS method. Two laser foci are placed along the x axis separated by a distance of 6 μm and record the time-resolved fluorescence intensities $I_1(t)$ and $I_2(t)$. The forward cross correlation of these two signals yields $G(t)$. Two foci are scanned simultaneously along the z axis to probe the velocity profile $v(z)$.

To determine the velocity profile we have scanned the foci position across the channel. The acquisition time was either 30 or 60 s, necessitating longer measurements close to the channel walls, where small flow velocities are found. Indeed, consider the worst case when the foci are centered on the wall. Since the concentration in particles is about 1 per femtoliter, the number of particles carried by the shear flow which enter the focus half-elliptical area during 60 s is about 6×10^4. At each z position, a series of 10 independent data acquisitions was carried out, so that $N \sim 6 \times 10^5$ particles were considered [19]. This gives a satisfactory signal to noise ratio $\sqrt{N}$ of order 10^3. The cross correlation functions acquired at position z were fitted with a Gaussian function for more precise determination of $\tau_M(z)$, yielding the particle velocity $v(z) = \Delta s/\tau_M(z)$, where Δs is the distance between foci. For every salt concentration, we have repeated experiments several times with freshly prepared channels and varied the pressure gradient.

A typical measured velocity profile is shown in Fig. 2. As expected, in the central region where the velocity of the tracer particles reflects that of the liquid [18], the profile exhibits the parabolic shape predicted by the classical theory. However, when foci presumably enter the wall, this parabola does not turn to zero by giving a plateau of nonzero constant velocity. This is observed for both hydrophobic and hydrophilic surfaces. The apparent velocity at

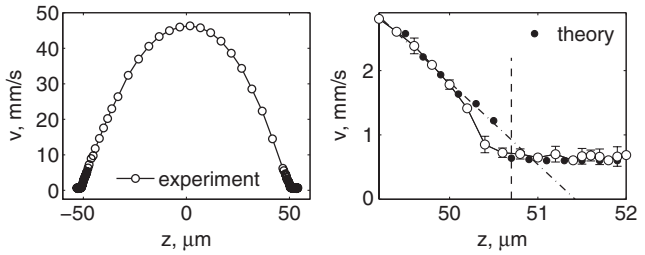

FIG. 2. Left panel: Typical velocity profile $v(z)$ (open circles) measured in a ~100 μm channel with 10^{-4} mol/L NaCl solution. Right panel: The same profile in the vicinity of the wall. Error bars were determined from the deviation among repeated measurements. When error bars are absent, uncertainties are smaller than the circles. The dots are simulation results. The dash-dotted line fits the data (the apparent slip length, $b_{app} \sim$ 740 nm), and the dashed line shows the wall location ($z =$ 50.69 μm).

the plateau region depends on added salt and hydrophobicity as shown in Fig. 3.

The apparent velocity at the wall is too large to reflect the true liquid slippage over it. Earlier estimates [18] suggested that in the vicinity of the wall, the tracers are submitted to a Taylor dispersion; i.e., their diffusion combined with shear enhances the migration speed in the flow direction. Now we model this effect precisely. Like in [18] we assume an ergodic system and interpret the time cross correlation $G(\tau)$ as

$$G(\tau) = \frac{\iint i_1(\boldsymbol{r}) i_2(\boldsymbol{r}') \Phi(\boldsymbol{r}, \boldsymbol{r}', \tau) d^3\boldsymbol{r} d^3\boldsymbol{r}'}{\bar{C}^2 \iint i_1(\boldsymbol{r}) i_2(\boldsymbol{r}') d^3\boldsymbol{r} d^3\boldsymbol{r}'}, \quad (1)$$

where $\boldsymbol{r} = (x, y, z)$, $\boldsymbol{r}' = (x', y', z')$, and the average concentration of labeled particles is denoted by $\bar{C}$. The real-space detection efficiencies $i_1(\boldsymbol{r})$ and $i_2(\boldsymbol{r})$ for focus 1 and 2 were given as ellipsoidal Gaussian functions. The function Φ is given as the solution of the advection-diffusion equation from a point source in a flow field with uniform velocity. In the vicinity of the wall, the particles are repelled by an electrostatic force, F, so that they do not completely fill up the ellipsoidal Gaussian lightened region. Keeping the same notation for the light intensity, we thus replace $i_1(\boldsymbol{r})$ by $i_1(\boldsymbol{r}) c_e(\boldsymbol{r})$, where $c_e(\boldsymbol{r})$ is the particle equilibrium concentration profile at the upstream focus, to be detailed below. The advection-diffusion equation to be solved for the concentration c is

$$\partial c_\tau + (\lambda z + b)\partial c_x + \partial (wc)_z = D\nabla^2 c, \quad (2)$$

where $w = F/(6\pi R\mu)$ is the migration velocity of a particle along z in a fluid of viscosity μ and D is the Einstein diffusion coefficient. Here we neglect the hydrodynamic interactions between the particles and wall. Since the distance from the wall $h \gg R$, the energy of electrostatic interaction of a particle with the wall is $U = q\phi_1 \exp(-\kappa h)$; i.e., the particle is considered as a point charge q (correspondingly, $F = -dU/dh$ [20]). Here ϕ_1 is the surface potential of the wall at the given concentration of the electrolyte with an inverse Debye length κ. The charge is given by $q = 4\pi R^2 q_s = 4\pi R \epsilon_0 \epsilon \phi_2 (\kappa R + 1)$, where q_s is the surface charge density, and ϕ_2 is the surface potential of the particle. Then, according to the Boltzmann law, the equilibrium concentration of particles in the vicinity of the wall is $c_e(\boldsymbol{r}) = c_0 \exp(-A \exp(-\kappa h))$, where $A = 4\pi R \phi_1 \phi_2 \epsilon_0 \epsilon (1 + \kappa R)/(k_B T)$. It has recently been proven [23] that the surface potential of a similarly silanized surface is close to that of glass, so that for ϕ_1 we use the data of [24]. Data for ϕ_2 were always smaller according to electrokinetic measurements, which are known to be a good estimate for a surface potential in case of hydrophilic surfaces. With these parameters, the values of A were of the order of 20 or smaller. Instead of solving for an initial point source, multiplying by $i_1(\boldsymbol{r}) c_1(\boldsymbol{r})$ and calculating the integral on $\boldsymbol{r}$ like in the numerator of Eq. (1), we may from the linearity of Eq. (2) solve for the initial cloud of illuminated particles with concentration $i_1(\boldsymbol{r}) c_1(\boldsymbol{r})$. The result $c(\boldsymbol{r}, \tau)$ is then multiplied by $i_2(\boldsymbol{r}')$ and integrated. This integral goes through a maximum at some time τ_M, which is interpreted as the transit time between foci, like in Fig. 1. Typical distributions of the concentration c_e and the intensity i_1 are shown in Fig. 4. For simplicity, we have reduced the 3D problem to a 2D one by integrating Eq. (2) along y. Then we obtain for $\bar{c} = \int_{-\infty}^{\infty} c dy$ an equation of the same form, with now $\nabla^2 = \partial^2_{x^2} + \partial^2_{z^2}$. The nonpenetration condition $\partial_z c = 0$ applies automatically at the wall as a result of the repulsive electrostatic force. The advection-diffusion equation was solved with a commercial finite elements software (COMSOL). The calculated τ_M provided the apparent transfer velocity between foci, $\Delta s/\tau_M$.

Introducing a shear rate of 1750 s^{-1} in (2) was necessary to obtain a profile with $\lambda \sim 1300$ s^{-1} fitting the experimental profile away from the wall. Our calculations then reproduce both the velocity profile away from the wall and

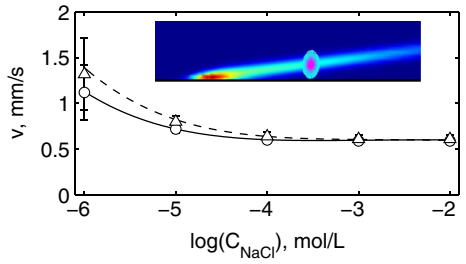

FIG. 3 (color online). The apparent velocity at the plateau region, v_{app}, at the hydrophobic wall (triangles) and hydrophilic wall (circles) as a function of concentration of NaCl. The concentration 10^{-6} mol/L corresponds to a case of pure water. The dashed and solid curves show the values predicted for $b = 100$ nm and $b = 0$, correspondingly ($\lambda \sim 1300$ s^{-1}). The inset shows typical calculated isoconcentration lines ($\bar{c}(x, z) = \mathrm{Ct}$) distorted by dispersion together with isolines of light intensity profile at the downstream focus ($\overline{i_2}(x, z) = \mathrm{Ct}$).

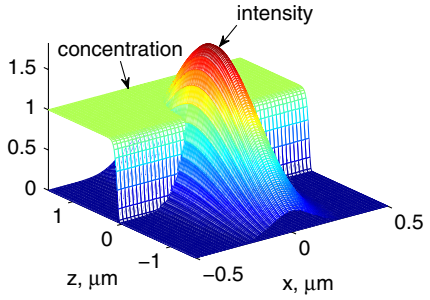

FIG. 4 (color online). Concentration at the upstream focus from the balance of Brownian motion and electrostatic repulsive forces for the typical case of 10^{-4} mol/L NaCl, and intensity at the upstream focus when centered at 100 nm from the wall. The concentration of illuminated particles is the product of these quantities.

the plateau region (see Fig. 2). At the vicinity of the wall there is some discrepancy between theoretical and experimental data, which suggests that nanoparticles are moving slower than predicted by the theory. This is likely due to a hindered diffusion owing to hydrodynamic effects ignored in our model. For this reason, only points at a distance larger than 600 nm were kept and straight lines were fitted through theoretical and experimental points. The fitted points in electrolyte solutions were at a distance from the wall larger than the expected range of electrostatic repulsive forces, so that it is unaffected by these. In each case, the intersection of the fitted line and of the plateau line gave a z reference point. Superimposing these points for a given concentration of salt (see Fig. 2), we determined a position of the wall in the experiment. An apparent slip length was then obtained by comparing the wall position and the zero velocity position in the experiment. The main experimental error, due to the electro-micromechanical positioning along z, was estimated as 30 nm. The fitting of experimental points suggests it is somewhat larger, and this is again attributed to the mechanical setup. The apparent slip lengths at the hydrophilic walls were found to be 740 nm for all electrolyte solutions. As shown by our calculation, these large observed values of the apparent slip at the hydrophilic wall are fully attributed to a Taylor dispersion of nanotracers. In the case of pure water, we were faced with difficulties in fitting due to a larger noise of both theoretical and experimental curves and the impossibility to determine the exact position of the wall (since the range of electrostatic repulsions from the wall is comparable to the focus size): the apparent slip was ca. 1 μm.

The velocity profiles calculated for a slip wall are fully consistent with data obtained near hydrophobic surfaces, and the apparent slip at the hydrophobic wall is found to be 60–70 nm larger than in case of a hydrophilic wall for all salt concentrations. It follows from our modelling that the contributions of the Taylor dispersion for the no slip and slip situations are of the same order, so that the difference of the apparent slip lengths is close to the actual ones. Alternatively, the true hydrophobic slip length was determined by comparing the apparent velocities at plateau regions (see Fig. 3). This procedure does not suffer from possible errors introduced by fitting and even does not depend on the choice of the wall location. Figure 3 shows that the results for hydrophobic surfaces are always below the curve computed for $b = 100$ nm. Again, we were unable to get very accurate data for pure water and observed a large scatter in the plateau values.

In the examples used above, the shear rate close to the wall was larger than in [16,17] and comparable to [12]. By varying the shear rate near the wall we found that it influences the value of the apparent slip. However, the true hydrophobic slip length remains the same.

In summary, we have performed a study of a flow of water-electrolyte solutions in microchannels coupled to a theoretical estimate of Taylor dispersion. Our approach allowed us to reduce dramatically an error in measurements as compared with known velocimetry methods due to orders of magnitude better statistics. Our results are in favor of no-slip boundary conditions for a hydrophilic surface. We have also demonstrated that there is a hydrophobic slip, of which the length does not exceed 80–100 nm, regardless of the variations of salt and shear rate.

[1] O. I. Vinogradova, Int. J. Miner. Process. **56**, 31 (1999).
[2] M. Z. Bazant and O. I. Vinogradova, J. Fluid Mech. **613**, 125 (2008).
[3] P. A. Thompson and S. M. Troian, Nature (London) **389**, 360 (1997).
[4] O. I. Vinogradova, Langmuir **11**, 2213 (1995).
[5] D. Andrienko, B. Dünweg, and O. I. Vinogradova, J. Chem. Phys. **119**, 13106 (2003).
[6] L. Bocquet and J. L. Barrat, Soft Matter **3**, 685 (2007).
[7] O. I. Vinogradova and G. E. Yakubov, Langmuir **19**, 1227 (2003).
[8] C. Cottin-Bizonne, B. Cross, A. Steinberger, and E. Charlaix, Phys. Rev. Lett. **94**, 056102 (2005).
[9] L. Joly, C. Ybert, and L. Bocquet, Phys. Rev. Lett. **96**, 046101 (2006).
[10] O. I. Vinogradova and G. E. Yakubov, Phys. Rev. E **73**, 045302(R) (2006).
[11] C. D. F. Honig and W. A. Ducker, Phys. Rev. Lett. **98**, 028305 (2007).
[12] P. Huang, J. Guasto, and K. Breuer, J. Fluid Mech. **566**, 447 (2006).
[13] E. Lauga, M. P. Brenner, and H. A. Stone, *Handbook of Experimental Fluid Dynamics* (Springer, New York, 2007), Chap. 19, pp. 1219–1240.
[14] R. G. Horn, O. I. Vinogradova, M. E. Mackay, and N. Phan-Thien, J. Chem. Phys. **112**, 6424 (2000).
[15] R. Pit, H. Hervet, and L. Leger, Phys. Rev. Lett. **85**, 980 (2000).
[16] D. C. Tretheway and C. D. Meinhart, Phys. Fluids **14**, L9 (2002).
[17] P. Joseph and P. Tabeling, Phys. Rev. E **71**, 035303(R) (2005).
[18] D. Lumma *et al.*, Phys. Rev. E **67**, 056313 (2003).
[19] To the best of our knowledge in the μ-PIV [17] and TIRV [12] methods, a maximum of $N \sim 10^3$ particles are normally analyzed in a control volume.
[20] Since one of the surfaces (of a polystyrene sphere) is always hydrophilic, we do not have any additional attractive force due to a formation of a gas bridge [21], which is observed between two hydrophobic surfaces [22].
[21] D. Andrienko, P. Patricio, and O. I. Vinogradova, J. Chem. Phys. **121**, 4414 (2004).
[22] G. E. Yakubov, H. J. Butt, and O. I. Vinogradova, J. Phys. Chem. B **104**, 3407 (2000).
[23] C. I. Bouzigues, P. Tabeling, and L. Bocquet, Phys. Rev. Lett. **101**, 114503 (2008).
[24] W. A. Ducker, T. Senden, and R. M. Pashley, Langmuir **8**, 1831 (1992).